Bioresource Technology 197 (2015) 227–234

Contents lists available at ScienceDirect

Bioresource Technology

journal homepage: www.elsevier.com/locate/biortech

Microbial community structure and function in response to the shift of sulfide/nitrate loading ratio during the denitrifying sulfide removal process

Cong Huang [a], Zhi-ling Li [a], Fan Chen [a], Qian Liu [a], You-kang Zhao [a], Ji-zhong Zhou [c,d], Ai-jie Wang [a,b,*]

[a] State Key Laboratory of Urban Water Resource and Environment, Harbin Institute of Technology, Harbin 150090, PR China
[b] Key Laboratory of Environmental Biotechnology, Research Center for Eco-Environmental Sciences, Chinese Academy of Sciences, Beijing 100085, PR China
[c] Institute for Environmental Genomics, Department of Microbiology and Plant Biology, University of Oklahoma, Norman, OK 73019, USA
[d] Earth Science Division, Lawrence Berkeley National Laboratory, Berkeley, CA 94270, USA

HIGHLIGHTS

- Optimized S^{2-}/NO_3^- (S/N) molar ratio was 5/6 for S^0 recovery and nitrate removal.
- Bacterial community and genetic activity remarkably modified as S/N ratio altered.
- Desulfurization and denitrification genera was predominant at S/N ratio of 5/6.
- Autotrophic S^{2-} oxidization genera dominated and functioned under lower S/N ratios.
- NO_3^- reduction and S^0 over oxidization genera functioned with higher S/N ratios.

GRAPHICAL ABSTRACT

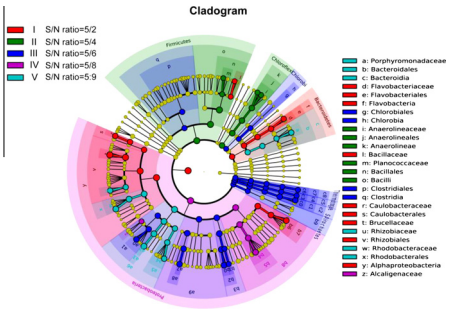

ARTICLE INFO

Article history:
Received 2 July 2015
Received in revised form 4 August 2015
Accepted 8 August 2015
Available online 12 August 2015

Keywords:
Denitrifying sulfide removal process
Continuous stirred tank reactor (CSTR)
Sulfide/nitrate loading ratio
Microbial community structure
Function

ABSTRACT

Influence of acetate-C/NO_3^--N/S^{2-} ratio to the functional microbial community during the denitrifying sulfide removal process is poorly understood. Here, phylogenetic and functional bacterial community for elemental sulfur (S^0) recovery and nitrate (NO_3^-) removal were investigated with the switched S^{2-}/NO_3^- molar ratio ranged from 5/2 to 5/9. Optimized S^{2-}/NO_3^- ratio was evaluated as 5/6, with the bacterial genera predominated with *Thauera*, *Enterobacter*, *Thiobacillus* and *Stappia*, and the *sqr* gene highly expressed. However, insufficient or high loading of acetate and NO_3^- resulted in the low S^0 recovery, and also significantly modified the bacterial community and genetic activity. With S^{2-}/NO_3^- ratio of 5/2, autotrophic S^{2-} oxidization genera were dominated and NO_3^- reduction activity was low, confirmed by the low expressed *nirK* gene. In contrast, S^{2-}/NO_3^- ratio switched to 5/8 and 5/9 introduced diverse heterotrophic nitrate reduction and S^0 over oxidization genera in accompanied with the highly expressed *nirK* and *sox* genes.

1. Introduction

Nitrate and sulfide compounds are frequently detected in sewerage, refinery and pharmaceutical industry (Show et al., 2013; Yuan et al., 2014). They gave rise to the serious contamination in

* Corresponding author at: State Key Laboratory of Urban Water Resource and Environment, Harbin Institute of Technology, Harbin 150090, PR China. Tel./fax: +86 451 86282195.
E-mail address: waj0578@hit.edu.cn (A.-j. Wang).

http://dx.doi.org/10.1016/j.biortech.2015.08.019
0960-8524/

many well-known forms based on their varied valent states – ammonia, nitrous acid, nitrate (NO_3^-), sulfate, sulfur dioxide, sulfide (S^{2-}), elemental sulfur (S^0) and etc. (Pikaar et al., 2014; Pokorna and Zabranska, 2015); among all of them, S^{2-} and NO_3^- are the most common forms as contaminants. When both S^{2-} and NO_3^- were present, sulfide oxidizing bacteria (SOB) was able to transfer S^{2-} to S^0 by utilizing NO_3^- as an electron acceptor, called the denitrifying sulfide removal (DSR) process (Wang et al., 2005); and the process supplies an effective means to recovery S^0 and simultaneous transfer of NO_3^- to nitrogen gas (N_2) from wastewater (Chen et al., 2008a).

Therefore, the extensive studies have conducted on the simultaneous removal of organic carbon, sulfite and nitrate (Chen et al., 2008a; Pokorna and Zabranska, 2015), focused on the high S^0 recovery rate under the different operating conditions and C/N/S ratios. Cai et al. (2008) reported that the S/N molar ratio controlled at 5/2 effectively improved the removal rates of S^{2-} and NO_3^- compared to the S/N ratios of 5/5 and 5/8 in anoxic sulfide oxidizing (ASO) reactors, and however, the S^0 recovery rate could not be guaranteed. Chen et al. (2008a) testified the S^0 recovery rate with C/N molar ratio ranged from 0.85/1, 1.05/1, 1.26/1 and 2/1 in expanded granular sludge blanket (EGSB) reactor, and found over 90% of S^0 recovery rate was obtained under the optimized condition. Cardoso et al. (2006) reported that the S^0 generation rate was gradually decreased with the increase of S/N molar ratio under the fixed C/N molar ratio of 1/1 in an upflow anaerobic sludge blanker (USAB) reactor. Lee and Wong (2014) evaluated the stoichiometry and kinetics of DSR process based on eight SOB isolated strains and a mixed microbial consortium, and found that the influent S/N and C/N molar ratio plays key roles in obtaining the high recovery of S^0 and simultaneously removal of NO_3^- and S^{2-}.

Practical S^{2-} and NO_3^- contaminated wastewater were varied in carbon source, e^--donor and e^--acceptor, so it is meaningful to estimate the functions of microbial communities and genetic activities upon the varied organic carbon/e^--donor/e^--acceptor ratios for optimization of S^0 recovery efficiency and stability. Microbial community structures during DSR process have been previously analyzed by PCR-DGGE and clone libraries (Cardoso et al., 2006; Chen et al., 2008b), but these researches only provided the restricted microbial community information. In addition, the variations of bacterial composition and putative functional genes related to sulfur oxidization and denitrification in response to different organic carbon/S^{2-}/NO_3^- loading ratio are little understood. The 454 pyrosequencing and quantitative reverse transcription-PCR (*q*RT-PCR), two recently developed technics respectively focused on 16S rRNA gene with a high taxonomic resolution and the quantitative analysis of genetic expression, are considered to be suitable for characterizing microbial community structure and functional genes during the DSR process (Andersson et al., 2009; Mahmood et al., 2009).

In this study, the S^0 recovery and denitrification efficiencies by the shift of acetate (Ac-C) and NO_3^- vs. S^{2-} ratio were investigated and the microbial phylogenetic and functional communities under the different loading ratios were characterized in the continuous stirred tank reactor (CSTR) using 16S rRNA 454 pyrosequencing and *q*RT-PCR. To guarantee the complete heterotrophic denitrification of NO_3^- to nitrogen gas, the Ac-C/NO_3^--N ratio (mol/mol) was controlled at 1/2, as confirmed by Lee and Wong (Lee and Wong, 2014). Therefore, Ac-C/NO_3^- ratio (mol/mol) was fixed at 1/2 and the S^{2-}/NO_3^--N ratios were ranged from 5/2 to 5/9. The objectives of this study were to (i) determine the impact of Ac-C and NO_3^- vs. S^{2-} ratio on elemental sulfur recovery and denitrification efficiency and (ii) identify the variation law of bacterial community composition and functional genes in response to the shift of Ac-C/NO_3^--N/S^{2-} ratio.

2. Method

2.1. Experimental set up

Five identical CSTRs with effective volume of 1.2 L were operated under the fixed Ac-C/NO_3^- ratio of 1/2 and S^{2-}/NO_3^- ratio of 5/2 (C-I), 5/4 (C-II), 5/6 (C-III), 5/8 (C-IV) and 5/9 (C-V), respectively. The running parameters were shown in details in Table 1. The reactors were wrapped with electrothermal wire to keep a consistent operating temperature of 30 ± 1 °C. Initially, the reactors were inoculated with an equal volume of sludge (0.3 L, 19 g TSS/L) from the anaerobic sludge thickener at WenChang Wastewater Treatment Plant (Harbin, China), and then they were kept running at the different Ac-C/NO_3^-/S^{2-} ratios with the intermittent mix at the rate of approximately 150 rpm. The trace element solution was continuously fed into the influent with a plunger pump (iPump2S, Baoding, China), with the detailed chemical composition described by Chen et al. (2008a). Bicarbonate (1 g L^{-1}) was employed to maintain the influent pH of 8.0 ± 0.3. All of the CSTR reactors were operated at a fixed HRT of 24 h. Concentration of Ac-C, NO_3^- and S^{2-} were determined at intervals until the reactors treatment efficiency achieved the steady state after more than 20 days.

2.2. Analytical methods

After achieved the steady state, influent and effluent samples (3–10 mL) were collected from inlet and outlet of the reactor and concentrations of acetate, NO_3^-, S^{2-}, SO_4^{2-} and S^0 were continuously analyzed. The pH and oxidation–reduction potential (ORP) of liquid samples inside the reactor were determined with a pH/ORP meter (FE20; Merrler Toledo, Switzerland). TSS was determined according to the standard methods (APHA, 1998). Concentrations of H_2S, HS^{-1} and S^{2-} were determined according to the methylene blue method (Trüper and Schlegel, 1964). Concentrations of sulfate (SO_4^{2-}), thiosulfate ($S_2O_3^{2-}$), sulfite (SO_3^{2-}), nitrate (NO_3^-) and nitrite (NO_2^-) were measured by an ion chromatography (ICS-90A; Dionex, USA) with the column (Ion-Pac AG4A AS4A-SC 4 mm, Dionex, USA) after filtrated with the Millipore filter of 0.45 μm. S^0 was analyzed according to the method descried by Jiang et al. (2009). Briefly, elemental sulfur and sulfite were converted to thiosulfate at high pH, which was analyzed for $S_2O_3^{2-}$ by ion chromatograph. The final concentration of S^0 was calculated from the concentration of $S_2O_3^{2-}$ according to the reaction stoichiometry.

2.3. DNA extraction and 454 pyrosequencing

After continuous running for about 50 days, samples (3–10 mL) were harvested from the middle of the five reactors with a sterilized sample spoon and stored in a 50 mL sterile plastic test tubes at −80 °C before went for DNA and RNA analysis. DNA was extracted using the PowerSoil DNA Isolation kit (MoBio Laboratories Inc, USA) according to the manufacturer's instructions. Concentration and purity of the extracted DNA were measured with Nanophotometer (P-class, Implen, Germany). Bacterial V1-V3 region of 16S rRNA gene was amplified using the forward primer 8F (5′-AGAGTTTGATCCTGGCTCAG-3′) and reverse primer 533R (5′-TTACCGCGGCTGCTGGCAC-3′). PCR products were purified using GeneJET™ PCR purification kit (Fermentas, USA) and then went for pyrosequencing on the 454 Genome Sequencer FLX platform. The sequences obtained from 454 pyrosequencing were analyzed following the pipelines of Quantitative Insights into Microbial Ecology (QIIME) software (www.microbio.me/qiime) as described by the previous studies (Caporaso et al., 2010; Loudon et al., 2014). Taxonomic classification of each phylotype was determined

Table 1
Operational conditions of five CSTRs.

CSTRs	Acetate Influent (mg L^{-1})	NO_3^- Influent (mg L^{-1})	S^{2-} Influent (mg L^{-1})	Ac-C/NO_3^--N ratio (moles/moles)	S^{2-}/NO_3^- ratio (moles/moles)
C-I	108.9 ± 8.7[a]	302.2 ± 16.0	202.1 ± 4.6	1/2	5/2
C-II	199.6 ± 11.7	659.0 ± 32.2	202.7 ± 3.9	1/2	5/4
C-III	310.3 ± 11.5	961.2 ± 30.3	201.7 ± 5.0	1/2	5/6
C-IV	395.6 ± 11.3	1260.9 ± 23.0	201.3 ± 4.2	1/2	5/8
C-V	510.7 ± 14.8	1490.6 ± 27.1	203.3 ± 4.8	1/2	5/9

[a] The data was the average measured results from triplicate samples with the standard deviation shown on the right side of "±".

using the SILVA rRNA database project with over 97% of sequence similarity, as suggested by Wang et al. (2007). The 16S rRNA gene sequence data were deposited in NCBI Sequence Read Archive under the accession number of SRR2136643.

2.4. RNA isolation and quantitative reverse transcription-PCR (qRT-PCR)

The total RNA was extracted using RNA PowerSoil™ Total RNA Isolation Kit (MoBio Laboratories Inc, USA) in accordance with the manufacturer's instructions. RNA concentration and purity was measured with a Nanophotometer (P-class, Implen, Germany). The total RNA of 2 μg was reversely transcribed using PrimeScript™ II 1st Strand cDNA Synthesis Kit (TaKaRa, Japan) following manufacturer's instruction. Concentration and purity of the cDNA were measured with Nanophotometer (P-class, Implen, Germany). The *q*RT-PCR was performed on an ABI 7500TM Real-Time PCR System (Applied Biosystems, CA, USA). Gene encoding sulfide quinone reductase (*sqr*) during sulfur oxidation process was amplified using the specific primer pairs of sqrF (GCTCGGCAGCCTCAATAC) and sqrR (GGTCGGACGGTGGTTACTG) (Yin et al., 2014). *NirK* gene encodes the copper-containing nitrite reductase during nitrate reduction process. This enzyme played an important role when nitrate reduced into nitrite. *Nirk* gene was detected by specific primer pairs of F1aCu (ATCATGGTSCTGCCGCG) and R3Cu (GCCTCGATCAGRTTGTGGTT) (Throbäck et al., 2004). *SoxB* gene, encoding SoxB subunit of the Sox enzyme system, considered as a fundamental and primordial molecular mechanism for sulfur oxidation, which oxidize sulfide, elemental sulfur and thiosulfate to sulfate. The specific primer sets for amplification of *soxB* gene were 710F (ATCGGYCAGGCYTTYCCSTA)/1184R (MAVGTGCCGTTGAARTTGC) (Tourna et al., 2014). The *q*RT-PCR mixture (25 μL) consisted of 1 × SYBR Green *q*PCR Mix (Tiangen, China), primer sets (200 nM for each) and about 3 ng of template cDNA. The PCR procedures for amplification of *sqr*, *soxB* and *nirK* genes were described in detail in the previous studies (Yin et al., 2014; Throbäck et al., 2004; Tourna et al., 2014). Calibration curves (log DNA concentration versus an arbitrarily set cycle threshold value) for *sqr*, *soxB* and *nirK* genes were constructed using serial dilutions of amplicons of single colonies. Gene copy number of the amplicon was calculated by multiplying the molar concentration of the amplicon by Avogadro's constant. Efficiencies of real-time PCR assays were over 95% and r^2 were 0.99. All experiments were performed in triplicates.

2.5. Statistical analysis

The richness estimator (Chao1) and diversity indices (Shannon and Simpson) were calculated using the DOTUR program. The Shannon index was calculated to estimate community diversity. The Shannon's diversity index is $H' = -\sum_{i=1}^{R} pi \log(pi)$, in which *pi* encoded the proportion of individuals belonging to the *i*th species in the data set of interest. It could be deduced from the formula that tags at low frequencies either from undetermined rare species or from experimental errors contribute little to the Shannon index, because *pi* value for rare tags is normally less than 10^{-3} for high-throughput sequencing results. Linear discriminant analysis (LDA) effect size (LefSe), a novel method to support the high dimensional class comparisons in metagenomics analysis (Zettler et al., 2013), was performed by the online LefSe program (http://huttenhower.sph.harvard.edu/galaxy/root?tool_id1/4lefse_upload). Significantly discriminant taxon nodes were colored and branch areas are shaded according to the highest-ranked variety for that taxon. Canonical correlation analysis (CCA) diagram, applied to describe correlations between community composition and environmental parameters, was performed by applying the R software (www.r-project.org).

3. Results and discussion

3.1. CSTR performances with the different S^{2-}/NO_3^- ratios

In this study, Ac-C/NO_3^- ratio was fixed at 1/2 to insure the complete transformation of NO_3^- to N_2 gas (Lee and Wong, 2014), and while, S^{2-}/NO_3^- ratios were altered to determine the optimized condition for S^0 recovery. In C-I (S^{2-}/NO_3^- ratio = 5/2; S^{2-}/Ac-C ratio = 5/1), acetate, NO_3^- and S^{2-} were completely removed, but the recovery rate of S^0 only achieved at 24.0%, accompanied with a large amount of SO_4^{2-} generated (153.5 mg L^{-1}) (Fig. 1). As the loading ratios of acetate and nitrate increased (C-II and C-III), S^0 generation rate was gradually improved and correspondingly, the produced SO_4^{2-} was decreased, which was probably caused by the increased electron acceptor (NO_3^-) supply for sulfide oxidization (Fig. 1 and Table 2). The highest yield of S^0 (84.4%) was observed at C-III. Here, the produced sulfate was the lowest (31.6 mg L^{-1}) and while, the removal rates of acetate, NO_3^- and S^{2-} were maintained at 100% (Fig. 1 and Table 2), indicating an optimal running condition with the balanced molar concentration of acetate, S^{2-} and NO_3^-. However, as the loading ratios of acetate and NO_3^- further increased (C-IV and C-V), neither acetate nor NO_3^- could be completely consumed (Table 2). Meanwhile, a large amount of SO_4^{2-} was generated and the S^0 generation rate was quickly dropped to 12.3% and 2.9% at C-IV and C-V, respectively. The above results gave information on the optimized S^{2-}/NO_3^- ratio of 5/6 when Ac-C/NO_3^- ratio was fixed at 1/2, and in contrast, S^{2-} over oxidization was occurred as the S^{2-}/NO_3^- ratio decreased or increased. Previously, Cai et al. (2008) evaluated the optimized S^{2-}/NO_3^- ratio as 5/2 for selectively generation of S^0 and N_2 gas, and however, the Ac-C/NO_3^- ratio was not clearly elaborated. Cardoso et al. (2006) discovered the depressed S^0 generation rate with the increase of S/N molar in a UASB reactor by fixing at C/N molar ratio of 1/1, but the removal rates of NO_3^- was not mentioned.

3.2. Bacterial diversity and community composition with the different S^{2-}/NO_3^- ratios

The 454 pyrosequencing was adopted to determine the abundance and diversity of bacterial populations in these reactors. Over 10,000 qualified sequences were produced with an average length of 450 bps for each bacterial community (Supplementary

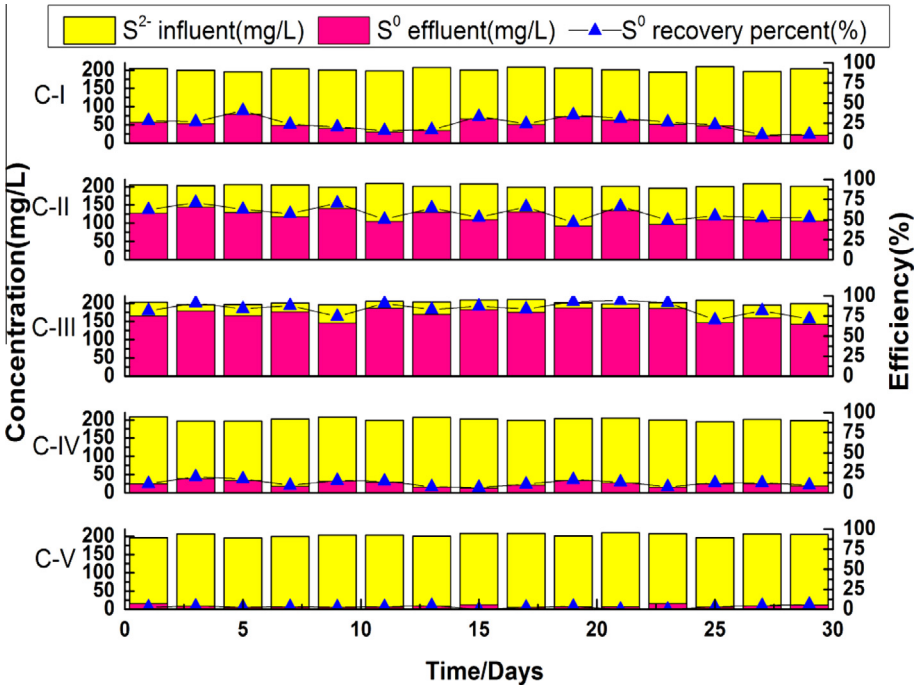

Fig. 1. Performances of S^0 recovery in CSTRs corresponding to the different S^{2-}/NO_3^- ratios. C-I: S/N ratio = 5/2, C-II: S/N ratio = 5/4, C-III: S/N ratio = 5/6, C-IV: S/N ratio = 5/8, C-V: S/N ratio = 5:9. The Ac-C/NO3$^-$-N ratio was kept at 1/2 under all the conditions.

Table 2
Performances at the steady running state in five CSTRs.

CSTRs	Acetate		NO_3^-		S^{2-}		SO_4^{2-}-S	S^0	
	Effluent (mg L^{-1})	Removal rate (%)[a]	Effluent (mg L^{-1})	Removal rate (%)	Effluent (mg L^{-1})	Removal rate (%)	Effluent (mg L^{-1})	Effluent (mg L^{-1})	Generation rate (%)[b]
C-I	0.0	100.0	0.0	100.0	0.0	100.0	153.5 ± 21.3	48.5 ± 22.1	24.0 ± 10.8
C-II	0.0	100.0	0.0	100.0	0.0	100.0	84.0 ± 16.7	118.7 ± 11.6	58.6 ± 8.1
C-III	0.0	100.0	0.0	100.0	0.0	100.0	31.6 ± 15.5	170.8 ± 15.7	84.4 ± 7.7
C-IV	53.2 ± 15.7[c]	86.6 ± 3.7	0.0	100.0	0.0	100.0	176.5 ± 9.4	24.7 ± 7.7	12.3 ± 4.0
C-V	167.0 ± 34.8	67.3 ± 6.9	135.8 ± 19.2	64.9 ± 5.0	15.1 ± 3.6	92.6 ± 1.7	182.4 ± 7.6	5.8 ± 3.5	2.9 ± 1.7

[a] Removal rate (%) was calculated by dividing the effluent concentration with the influent concentration.
[b] S^0 generation rate (%) was calculated by dividing the effluent concentration of S^0 with the concentration of S^{2-} in influent.
[c] The data was the average results from triplicate samples with the standard deviation shown on the right side of "±".

information Fig. S1). More than 35 types of bacterial genus were recovered altogether, and among all of them, bacterial communities in C-I and C-V have a relative higher diversity with Shannon indices of 3.31 and 4.04, respectively, compared with C-II, C-III and C-IV with Shannon indices varying from 2.02 to 2.73 (Table 3).

The obvious different bacterial composition was observed between C-I to C-V based on the different loading ratios of acetate and nitrite (Fig. 2). C-I sample was dominated with *Arcobacter* (20.8%), *Desulfobulbus* (14.9%) and *Thermovirga* (10.7%). Among of them, *Arcobacter* was able to oxidize sulfide autotrophically into filamentous sulfur and simultaneously fix carbon dioxide to organic compounds (Wirsen et al., 2002). *Thermovirga* was anaerobic sulfur reducing bacteria that utilizing organic acid as carbon source and electron donor (Göker et al., 2012), and *Desulfobulbus* was able to reduce both sulfate and sulfite (Laanbroek et al., 1984). Microbial community structures were similar in C-II to C-III, that predominated with *Thiobacillus* (31.5–31.6%), *Enterobacter* (27.2–4.8%), *Stappia* (13.4–26.7%), *Rhizobium* (4.0–7.0%), and *Thauera* (2.6–10.2%), respectively. Among of them, sulfide oxidization and denitrification bacteria which converted sulfide to S^0 and NO_3^- to N_2 were predominant, including genera of *Thauera*, *Enterobacter*, *Thiobacillus* and *Stappia* (Liu et al., 2006, 2015; Meyer et al., 2007; Schedel and Trüper, 1980). Bacterial community structures of C-IV and C-V were much different from the others, that C-IV was occupied with genera of *Ochrobactrum* (54.1%), *Stenotrophomonas* (16.7%) and *Flavobacterium* (10.4%), and while, C-V was predominant with genera of *Exiguobacterium* (61.8%), *Anaerolineaceae* (8.5%) and *Leptolinea* (3.9%). Of which, *Leptolinea*, *Exiguobacterium*, *Flavobacterium*, and *Ochrobactrum* were in charge of denitrification or sulfate reduction under heterotrophic condition (Frühling et al., 2002; Kitamikado et al., 1981; Mahmood et al., 2009; Yamada et al., 2006). These clear differences indicated

Table 3
Similarity-based OTUs, species richness and diversity estimation of the determined bacteria in samples of C-I to C-V.

Sample	Reads	OTU[a]	Coverage (%)	Chao	Shannon	Simpson
C-I	13,379	657	97.6	1245	3.31	0.2358
C-II	10,595	382	98.2	631	2.59	0.1698
C-III	10,976	432	98.1	764	2.73	0.1651
C-IV	11,683	338	98.5	586	2.02	0.2953
C-V	11,325	867	96.0	1650	4.04	0.0671

[a] The OTUs were classified with the sequence similarity over.

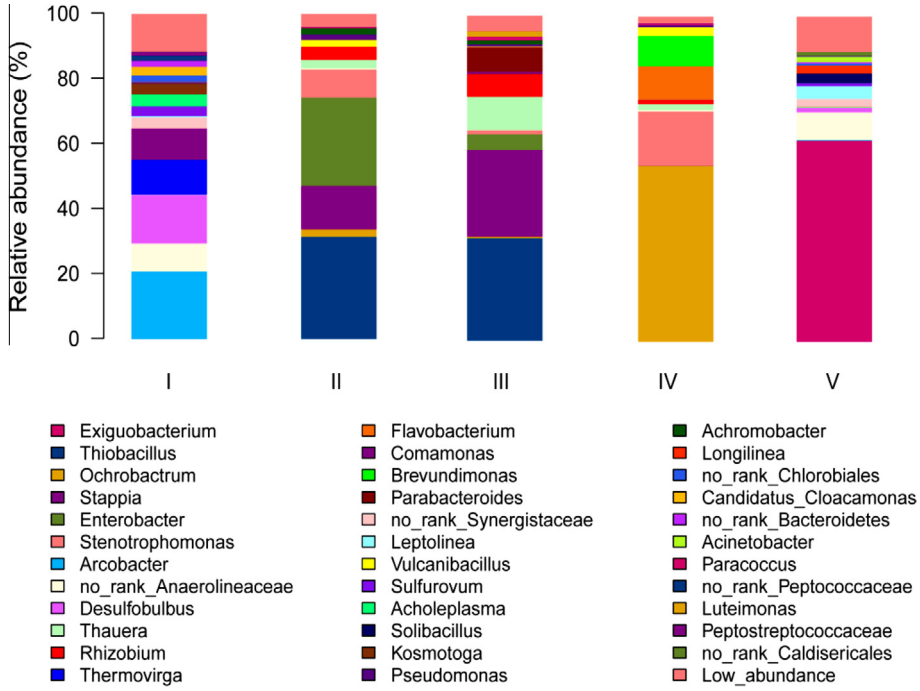

Fig. 2. Bacterial community structures in lever of genus in CSTRs corresponding to the different S^{2-}/NO_3^- ratios. I: S/N ratio = 5/2, II: S/N ratio = 5/4, III: S/N ratio = 5/6, IV: S/N ratio = 5/8, V: S/N ratio = 5:9. The Ac-C/NO_3^--N ratio was kept at 1/2 under all the conditions.

the variation of acetate and nitrate loading ratio markedly influenced the bacterial diversity and community composition.

3.3. LefSe analysis of bacterial community structures with the different S^{2-}/NO_3^- ratios

LefSe was adopted to obtain the more insights of the differentiation and internal interactions of the determined bacterial affiliation in samples C-I to C-V, with the taxonomic tree generated as shown in Fig. 3. The cladogram showed taxa with LDA values was higher than 4.0 for clarity (Fig. S2). Phylum *Proteobacteria* was predominated in C-II, C-III, C-IV and C-V, and while, *Bacteroidetes*, *Theromotogae* and *Spirochetes* were enriched in C-III, C-IV and C-V. In contrast, at the fine taxonomy levels, C-I were consisted of *Firmicutes* and *Chloroflex*. Although the communities in C-II and C-III were similar (Fig. 2), their bacterial lineages were different. In C-II, 6 fine lineages had an LDA value of 4 or higher in phylum of *Proteobacteria*, and family *Enterobacteriales* was also enriched. In comparison, sample C-III was consisted of families of *Hydrogenophilaceae*, *Rhodocyclaceae*, *Rhodobacteraceae*, *Rhizobiaceae*, and *Porphyromonadaceae*. LefSe highlighted the remarkable differences of bacterial community membership between samples C-I to C-V.

3.4. CCA diagram analysis

CCA diagram was applied to describe the correlations between the dominant bacterial genera and applied factors of acetate, NO_3^- and S^{2-} in samples C-I to C-V, as shown in Fig. 4. Dominated genera in C-I (including *Arcobacter*, *Desulfobulbus* and *Thermovirga*) located on negative direction of horizontal axis were negatively correlated with acetate and NO_3^-. On the contrary, C-IV and C-V affiliated genera, such as *Leptolinea*, *Exiguobacterium*, *Flavobacterium*, *Ochrobactrum*, were distributed in the direction lines (or the extension lines) of acetate and nitrate, indicating their involvement of the removals of acetate and NO_3^-. C-II and C-III affiliated genera, including *Thauera*, *Enterobacter*, *Thiobacillus* and *Stappia*, were distributed either along with or closed to sulfide line. The positive correlation of S^{2-} and the abundant genera, explains the improved S^0 yield rates at C-II and C-III samples.

3.5. Quantitative expression of denitrification and sulfide oxidation related genes with the different S^{2-}/NO_3^- ratios

The *q*RT-PCR was conducted to estimate the expressed functional genes, including *nirK*, *sqr* and *soxB*, during the denitrification and sulfide oxidation processes with samples C-I to C-V (Fig. 5). Efficiency values were 0.98, 0.97 and 0.98 for *nirK*, *sqr* and *soxB* genes, respectively, with R^2 value of 0.99. From C-I to C-V, the expressed *nirK* gene was gradually increased from log values of 3.1 to 11.8, indicated the enhanced denitrification activities based on the high loading ratios of NO_3^- and acetate. Sulfite oxidized to S^0 was targeted specifically using *sqr* gene. Expressed *sqr* gene was relatively higher in C-II (log value 5.1) and C-III (log value 6.9) compared with samples of C-I, C-IV and C-V, suggesting the high S^{2-} oxidization activity, which was coincident with the high recovery rate of S^0 in these two conditions (Fig. 1). In contrast, the expressed *sqr* genes in C-IV and C-V were much lower, with the log values of 1.4 and 0.9, reflecting the low S^{2-} oxidization activity. Presence of *soxB* gene was utilized as an indicator of oxidization of S^{2-}, S^0 and $S_2O_3^{2-}$ to SO_4^{2-}. The gradual increase of the expressed *soxB* gene stepwise from 3.6 to 6.4 (log value) from C-I to C-V manifested the gradual lifting activity of SO_4^{2-} generation as the loading ratios of electron acceptor (NO_3^-) and organic carbon (Ac-C) increased. QRT-PCR analysis further confirmed the high S^0 generation activity under C-II and C-III and the high denitrification and sulfate generation activities under C-IV and C-V.

3.6. Discussion

The DSR process has shown a great potential in wastewater treatment application, since it transfers S^{2-} and NO_3^- to completely water-insoluble S^0 and N_2 gas, and generates no secondary contaminant to water body (Chen et al., 2008a; Wang et al., 2005).

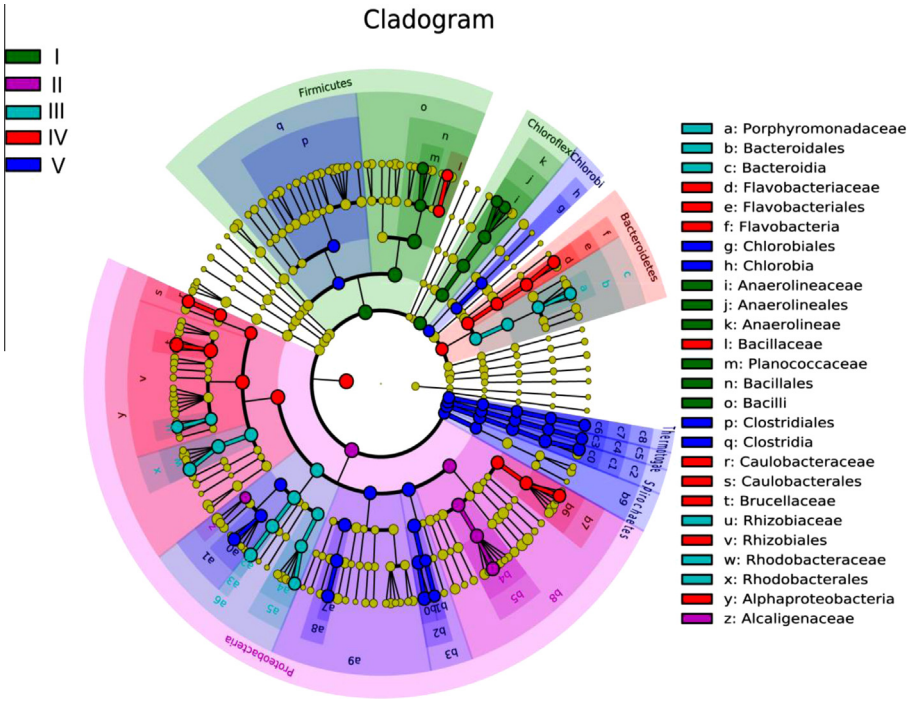

Fig. 3. Taxonomic tree generated using the LEfSe online software highlighting the biomarkers that statistically differentiated the samples under the different S^{2-}/NO_3^- ratios. I: S/N ratio = 5/2, II: S/N ratio = 5/4, III: S/N ratio = 5/6, IV: S/N ratio = 5/8, V: S/N ratio = 5:9. The Ac-C/NO_3^--N ratio was kept at 1/2 under all the conditions.

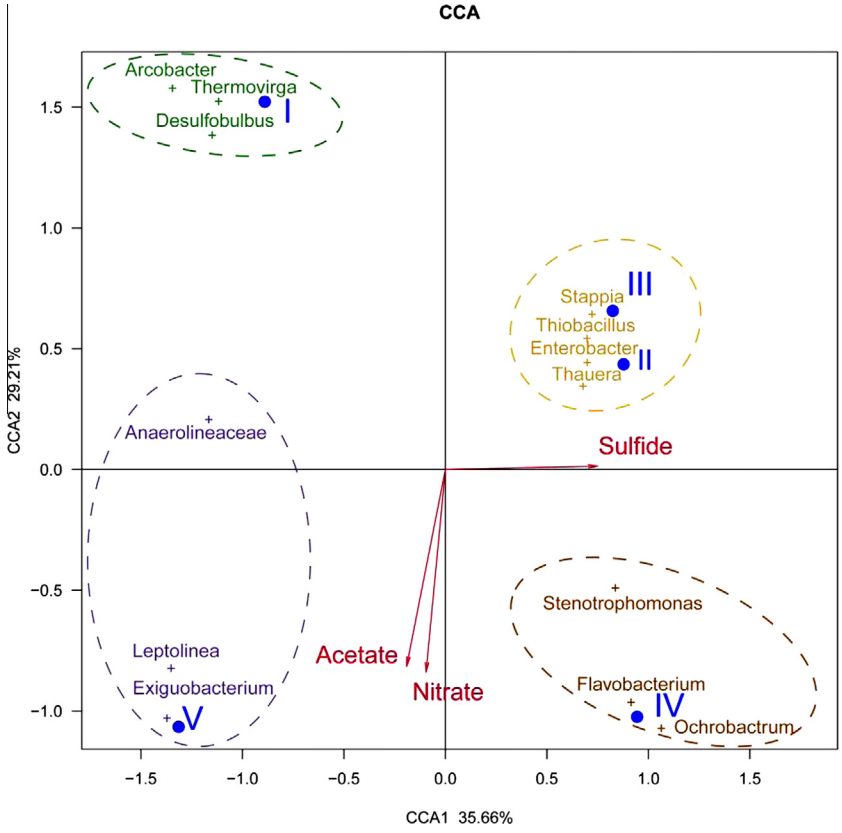

Fig. 4. Canonical correspondence analysis (CCA) comparing the correlations of bacterial community dynamics and applied acetate, NO_3^- and S^{2-} applied in the under five operational conditions. The eigenvalues of horizontal and vertical axes equal to CCA1 of 35.66% and CCA2 of 29.21%. Each sample is represented by blue point; each genus is represented by a colored point (green for C-I, yellow for C-II and C-III, purple for C-IV, and brown for C-V), accompanied by the genus name. Environmental variable are indicated by red lines with variable names (in red) at the end. (For interpretation of the references to color in this figure legend, the reader is referred to the web version of this article.)

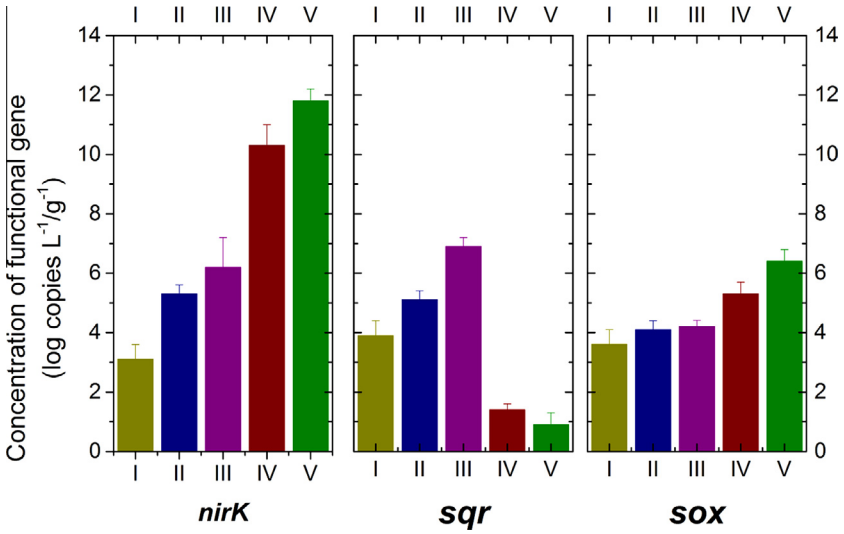

Fig. 5. Quantitative expression of denitrification and sulfide oxidation related genes, including nirK, sqr and soxB with the different S^{2-}/NO_3^- ratios. I: S/N ratio = 5/2, II: S/N ratio = 5/4, III: S/N ratio = 5/6, IV: S/N ratio = 5/8, V: S/N ratio = 5:9. The Ac-C/NO_3^--N ratio was kept at 1/2 under all the conditions.

However, on account of the alterable valent states and multiple redox potentials of both S and N, exploration of the effective solution to regulate the DSR process and avoid the unwanted or unnecessary biochemical reactions, like S^{2-} over oxidization or sulfite reduction, has become a tough issue urgently to be addressed. The previous studies majorly stressed on the physiological and kinetic behavior during nitrate removal and S^0 recovery (Chen et al., 2008a; Huang et al., 2015; Krishnakumar et al., 2005; Reyes-Avila et al., 2004), and however, functional microbes and genes in associated with S^{2-} and NO_3^- conversion processes were rarely concerned. For the first time, the study elaborated the bacterial community and genetic activity in response to the shift of Ac-C/NO_3^-/S^{2-} ratio. The analysis of bacterial abundance and diversity and functional genes confirmed that the shift of S^{2-}/NO_3^- ratio led to the obvious alteration of microbial community structure (Figs. 2–4) and genetic activity (Fig. 5) and gave hints on how the bacterial communities regulate the DSR process (Fig. 1 and Table 2).

S^0 yield rate was gradually improved as S^{2-}/NO_3^- ratio increased in C-II and achieved the highest at C-III. Meanwhile, removal rates of NO_3^- and acetate approached to 100% under these two conditions, suggested an optimized running condition with S^{2-}/NO_3^- ratio of 5/6 (Fig. 1 and Table 2) in this study. Here, the estimated bioprocesses and the potential function of these dominant genera were revealed as follows: first of all, most of dominate genera (*Thiobacillus*, *Enterobacter*, *Stappia*, and *Thauera*) in C-II and C-III (Figs. 2 and 4) were capable of oxidizing S^{2-} to S^0 applying NO_3^- as electron acceptor ($S^{2-} + 0.4NO_3^- + 1.2H_2O \rightarrow S^0 + 0.2N_2 + 2.4OH^-$) (Huang et al., 2015). The high quantity of expressed *sqr* gene in C-II and C-III, also confirmed the high activity of S^{2-} oxidization to S^0 compared with other conditions (Fig. 5). Meanwhile, nitrate may be participated in acetate degradation ($NO_3^- + 0.63CH_3COO^- + 0.37CO_2 \rightarrow 0.5N_2 + 0.13H_2O + 1.63HCO_3^-$), conducted by some nitrate reducing genera, like the dominant *Rhizobium* (Daniel et al., 1982). The expressed gene of *nirK* also confirmed the nitrate reducing activity (Fig. 5). Meanwhile, acetate could also be consumed by acidophilic methanogens ($CH_3COOH \rightarrow CH_4 + 4H_2O$) (Huang et al., 2015), although the archaea community was not elaborated here.

The insufficient or overloaded amount of acetate and nitrate resulted in the low S^0 recovery rate and large amount of sulfate generation (Fig. 1). When both acetate and nitrate were insufficient (C-I), S^0 was regarded as an energy storage polymer in prokaryotes. S^{2-} was conversed to S^0 and then further oxidized to SO_4^{2-} under autotrophic condition, which was conducted by the most abundant genera, *Arcobacter* and *Thermovirga* (Figs. 2 and 4). The hypothetical transformation equations were listed as follows: $xS^{2-} + yCO_2 + zH^+ \rightarrow xS^0 + y$ Organic carbon + $z/2H_2O$; $xS^0 + yCO_2 + zH_2O \rightarrow xSO_4^{2-} + y$ organic carbon + $2zH^+$ (Wirsen et al., 2002). The expressed *nirK* was the lowest in C-I (Fig. 5), confirmed the low nitrate reducing activity. Since *Desulfobulbus* were also dominant, it is estimated sulfate reduction was also possibly occurred ($SO_4^{2-} + CH_3COO^- + H^+ \rightarrow S^{2-} + 2CO_2 + 2H_2O$) (Laanbroek et al., 1984). The above results were supported by the positive expression of *sox* gene (Fig. 4).

As the loading ratios of acetate and NO_3^- were in excess (C-IV and C-V), genera of *Leptolinea*, *Exiguobacterium*, *Flavobacterium* and *Ochrobactrum* were the most abundant, indicated the predominate bioprocesses that nitrate reduction and the over oxidization of S^0 to SO_4^{2-} under heterotrophic conditions were the ($S^{2-} + 1.6NO_3^- + 1.6H^+ \rightarrow SO_4^{2-} + 0.8N_2 + 0.8H_2O$; $S^0 + 1.2NO_3^- + 0.4H_2O \rightarrow SO_4^{2-} + 0.6N_2 + 0.8H^+$) (Huang et al., 2015). Meanwhile, the expressed *nirK* and *sox* genes achieved the highest value in C-IV and C-V, further verified the lifting activities of nitrate reduction and SO_4^{2-} generation. A probable explanation is the rate of electron production from TCA cycle is slower than sulfide oxidization. The sulfur cycle could be a supplement electron donor for denitrification, since the complete sulfide oxidization could supply more electrons for denitrification (i.e., $S^{2-} \rightarrow S^0$, 2e; $S^{2-} \rightarrow SO_4^{2-}$, 8e).

4. Conclusion

The shift of S^{2-}/NO_3^--N molar ratio impacted the S^0 recovery rate and the removal rates of NO_3^- and acetate, and also significantly altered both the bacterial community structure and genetic activity. The optimized condition for S^0 recovery was determined with the SO_4^{2-}/NO_3^- ratio of 5/6 and the acetate-C/NO_3^--N ratio of 1/2, where the desulfurization and denitrification genera were dominant and *sqr* gene was highly expressed. The study gave suggestions for the effective control of the DSR process through the regulation of the bacterial communities.

Acknowledgements

This research was supported by the National Natural Science Foundation of China (NSFC, No. 31370157, No. 21407164,

No. 51408591 and No. 31400104), by National Science Foundation for Distinguished Young Scholars (Grant No. 51225802), by the National High-tech R&D Program of China (863 Program, Grant No. 2011AA060904), by the Major Science and Technology Program for Water Pollution Control and Treatment (No. 2014ZX07204-005), by "Hundred Talents Program" of the Chinese Academy of Sciences, by Project 135 of Chinese Academy of Sciences (No. YSW2013B06), and by Science and Technology Service Network Initiative of Chinese Academy of Sciences (No. KFJ-EW-STS-102).

Appendix A. Supplementary data

Supplementary data associated with this article can be found, in the online version, at http://dx.doi.org/10.1016/j.biortech.2015.08.019.

References

Andersson, A.F., Riemann, L., Bertilsson, S., 2009. Pyrosequencing reveals contrasting seasonal dynamics of taxa within Baltic Sea bacterioplankton communities. ISME J. 4 (2), 171–181.
APHA, 1998. Standard Methods for the Examination of Water and Wastewater, 20th ed. American Public Health Association, Inc., New York, USA.
Cai, J., Zheng, P., Mahmood, Q., 2008. Effect of sulfide to nitrate ratios on the simultaneous anaerobic sulfide and nitrate removal. Bioresour. Technol. 99 (13), 5520–5527.
Caporaso, J.G., Kuczynski, J., Stombaugh, J., 2010. QIIME allows analysis of high-throughput community sequencing data. Nat. Methods 7 (5), 335–336.
Cardoso, R.B., Sierra-Alvarez, R., Rowlette, P., 2006. Sulfide oxidation under chemolithoautotrophic denitrifying conditions. Biotechnol. Bioeng. 95 (6), 1148–1157.
Chen, C., Ren, N.Q., Wang, A.J., 2008a. Simultaneous biological removal of sulfur, nitrogen and carbon using EGSB reactor. Appl. Microbiol. Biotechnol. 78 (6), 1057–1063.
Chen, C., Wang, A.J., Ren, N.Q., 2008b. Biological breakdown of denitrifying sulfide removal process in high-rate expanded granular bed reactor. Appl. Microbiol. Biotechnol. 81 (4), 765–770.
Daniel, R.M., Limmer, A.W., Steele, K.W., 1982. Anaerobic growth, nitrate reduction and denitrification in 46 *Rhizobium* strains. Microbiology 128 (8), 1811–1815.
Frühling, A., Schumann, P., Hippe, H., 2002. *Exiguobacterium undae* sp. nov. and *Exiguobacterium antarcticum* sp. nov. Int. J. Syst. Evol. Micr. 52 (4), 1171–1176.
Göker, M., Saunders, E., Lapidus, A., 2012. Genome sequence of the moderately thermophilic, amino-acid-degrading and sulfur-reducing bacterium *Thermovirga lienii* type strain (Cas60314(T)). Stand. Genomic Sci. 6 (2), 230–239.
Huang, C., Zhao, Y., Li, Z., 2015. Enhanced elementary sulfur recovery with sequential sulfate-reducing, denitrifying sulfide-oxidizing processes in a cylindrical-type anaerobic baffled reactor. Bioresour. Technol. 192, 478–485.
Jiang, G., Sharma, K.R., Guisasola, A., 2009. Sulfur transformation in rising main sewers receiving nitrate dosage. Water Res. 43 (17), 4430–4440.
Kitamikado, M., Ito, M., Li, Y.T., 1981. Isolation and characterization of a keratan sulfate-degrading endo-beta-galactosidase from *Flavobacterium keratolyticus*. J. Biol. Chem. 256 (8), 3906–3909.
Krishnakumar, B., Majumdar, S., Manilal, V.B., 2005. Treatment of sulphide containing wastewater with sulphur recovery in a novel reverse fluidized loop reactor (RFLR). Water Res. 39 (4), 639–647.
Laanbroek, H.J., Geerligs, H.J., Sijtsma, L., et al., 1984. Competition for sulfate and ethanol among *Desulfobacter*, *Desulfobulbus*, and *Desulfovibrio* species isolated from intertidal sediments. Appl. Environ. Microbiol. 47 (2), 329–334.
Lee, D.J., Wong, B.T., 2014. Denitrifying sulfide removal by enriched microbial consortium: kinetic diagram. Bioresour. Technol. 164, 386–393.
Liu, B., Zhang, F., Feng, X., 2006. *Thauera* and *Azoarcus* as functionally important genera in a denitrifying quinoline-removal bioreactor as revealed by microbial community structure comparison. FEMS Microbiol. Ecol. 55 (2), 274–286.
Liu, L., Guo, Z., Lu, J., 2015. Kinetic model for microbial growth and desulphurisation with *Enterobacter* sp. Biotechnol. Lett. 37 (2), 375–381.
Loudon, A.H., Woodhams, D.C., Parfrey, L.W., 2014. Microbial community dynamics and effect of environmental microbial reservoirs on red-backed salamanders (*Plethodon cinereus*). ISME J. 8 (4), 830–840.
Mahmood, Q., Hu, B., Cai, J., 2009. Isolation of *Ochrobactrum* sp.QZ2 from sulfide and nitrite treatment system. J. Hazard. Mater. 165 (1–3), 558–565.
Meyer, B., Imhoff, J.F., Kuever, J., 2007. Molecular analysis of the distribution and phylogeny of the *soxB* gene among sulfur-oxidizing bacteria – evolution of the Sox sulfur oxidation enzyme system. Environ. Microbiol. 9 (12), 2957–2977.
Pikaar, I., Sharma, K.R., Hu, S., 2014. Reducing sewer corrosion through integrated urban water management. Science 345 (6198), 812–814.
Pokorna, D., Zabranska, J., 2015. Sulfur-oxidizing bacteria in environmental technology. Biotechnol. Adv. http://dx.doi.org/10.1016/j.biotechadv.2015.02.007.
Reyes-Avila, J., Razo-Flores, E.a., Gomez, J., 2004. Simultaneous biological removal of nitrogen, carbon and sulfur by denitrification. Water Res. 38 (14), 3313–3321.
Schedel, M., Trüper, H., 1980. Anaerobic oxidation of thiosulfate and elemental sulfur in *Thiobacillus denitrificans*. Arch. Microbiol. 124 (2–3), 205–210.
Show, K.-Y., Lee, D.-J., Pan, X., 2013. Simultaneous biological removal of nitrogen–sulfur–carbon: recent advances and challenges. Biotechnol. Adv. 31 (4), 409–420.
Throbäck, I.N., Enwall, K., Jarvis, Å., 2004. Reassessing PCR primers targeting *nirS*, *nirK* and *nosZ* genes for community surveys of denitrifying bacteria with DGGE. FEMS Microbiol. Ecol. 49 (3), 401–417.
Tourna, M., Maclean, P., Condron, L., 2014. Links between sulphur oxidation and sulphur-oxidising bacteria abundance and diversity in soil microcosms based on *soxB* functional gene analysis. FEMS Microbiol. Ecol. 88 (3), 538–549.
Trüper, H.G., Schlegel, H.G., 1964. Sulphur metabolism in *Thiorhodaceae* I. Quantitative measurements on growing cells of *Chromatium okenii*. Anton. Leeuw. Int. J. G. 30 (1), 225–238.
Wang, A.-J., Du, D.-Z., Ren, N.-Q., 2005. An innovative process of simultaneous desulfurization and denitrification by *Thiobacillus denitrificans*. J. Environ. Sci. Health A 40 (10), 1939–1949.
Wang, Q., Garrity, G.M., Tiedje, J.M., 2007. Naive Bayesian classifier for rapid assignment of rRNA sequences into the new bacterial taxonomy. Appl. Environ. Microbiol. 73 (16), 5261–5267.
Wirsen, C.O., Sievert, S.M., Cavanaugh, C.M., 2002. Characterization of an autotrophic sulfide-oxidizing marine *Arcobacter* sp. That produces filamentous sulfur. Appl. Environ. Microbiol. 68 (1), 316–325.
Yamada, T., Sekiguchi, Y., Hanada, S., 2006. *Anaerolinea thermolimosa* sp. nov., *Levilinea saccharolytica* gen. nov., sp. nov. and *Leptolinea tardivitalis* gen. nov., sp. nov., novel filamentous anaerobes, and description of the new classes *Anaerolineae classis* nov. and *Caldilineae classis* nov. in the bacterial phylum Chloroflexi. Int. J. Syst. Evol. Micr. 56 (6), 1331–1340.
Yin, H., Zhang, X., Li, X., 2014. Whole-genome sequencing reveals novel insights into sulfur oxidation in the extremophile *Acidithiobacillus thiooxidans*. BMC Microbiol. 14 (1), 179.
Yuan, Y., Chen, C., Liang, B., 2014. Fine-tuning key parameters of an integrated reactor system for the simultaneous removal of COD, sulfate and ammonium and elemental sulfur reclamation. J. Hazard Mater. 269, 56–67.
Zettler, E.R., Mincer, T.J., Amaral-Zettler, L.A., 2013. Life in the "Plastisphere": microbial communities on plastic marine debris. Environ. Sci. Technol. 47 (13), 7137–7146.